A Monte Carlo renormalisation group study of the two-dimensional discrete cubic model: a hint for superconformal invariance

1987 J. Phys. A: Math. Gen. 20 3425

(http://iopscience.iop.org/0305-4470/20/11/044)

J. Phys. A: Math. Gen. 20 (1987) 3425-3443. Printed in the UK

A Monte Carlo renormalisation group study of the two-dimensional discrete cubic model: a hint for superconformal invariance

R Badke

Universität Bonn Physikalisches Institut, Nussallee 12, D-5300 Bonn 1, Federal Republic of Germany

Received 22 October 1986, in final form 5 December 1986

Abstract. The discrete cubic model for six states of the lattice variables is investigated at one special point of the phase diagram where a number of contradicting results are known concerning the order of the phase transition and the critical exponents. A new implementation of the MCRG method is used for determining the critical point with great accuracy and for calculating the critical exponents. A continuous phase transition is found.

Following the recent results for six-state self-dual quantum chains with cubic symmetry where for a special point superconformal invariance is discovered, the critical exponents obtained are explained in the framework of this theory indicating a superconformal point with a conformal anomaly of $c = 1.25$.

1. Introduction

The cubic model (Aharony 1977, Kim *et al* 1975) is a generalisation of the widely known Ashkin-Teller model (Ashkin and Teller 1943) which is well understood (Ditzian *et al* 1980). The model exhibits a rich phase structure and has resisted an analytic solution so far. But from the analytical as well as from the numerical point of view there is a growing interest in the model.

The phase structure of the cubic model with six states for the lattice variables is roughly known. But the results of the various investigations with different methods disagree on the point of the order of the phase transitions. In a mean-field calculation Kim *et al* found a second-order phase transition (Kim *et al* 1975) and by applying the Bethe-Peierls-Weiss approximation Kim and Levy got a first-order transition (Kim and Levy 1975). The result of Nienhuis *et al* who performed an intensive study using a variational renormalisation group technique was again a first-order transition. A Monte Carlo calculation with a finite-size scaling analysis showed a second-order transition (Badke *et al* (1985a, b). The various contradicting results strongly motivate a new consideration of the model.

Another motivation comes from the formulation of the cubic model with six states as a finite quantum chain. Applying the theory of conformal invariance to a self-dual quantum chain with cubic symmetry von Gehlen and Rittenberg (1986) found a second-order phase transition and a plateau in the space of coupling constants where the corresponding conformal anomaly is constant with a value of about $c \approx 1.25$. For one of their points they discovered an additional $N = 1$ supersymmetry (von Gehlen and Rittenberg 1987). For another point of the general six-state model without cubic symmetry Zamolodchikov and Fateev (1985) suggested a conformal anomaly of $c = 1.25$

0305-4470/87/113425+19$02.50

using a larger algebra. For this point their conjectures are confirmed by a recent finite-size scaling investigation of Alcaraz (1986).

I present here a Monte Carlo renormalisation group (MCRG) study of the cubic model in the Lagrange formulation. Because of the known differences between the Lagrange and the Hamilton formulation it is interesting to test whether one can find results which can also be explained within the framework of superconformal invariance in the Lagrange formulation. Because of the enormous amount of computer resources which are required by the simulations in the Lagrange formulation I shall specialise in this paper to the critical point in the phase transition of the cubic model where most numeric results are available. The MCRG method is chosen for two reasons. Firstly it provides the possibility of calculating higher exponents in a simple manner. Secondly this model provides the possibility of applying new techniques in the implementation of the MCRG method. With the calculation of effective renormalised coupling constants (Swendsen 1984a, b, Gupta and Cordery 1984) one can approach the fixed point in a systematic way (Badke 1987) and use a new extrapolation procedure.

From the various experimental realisations of the discrete cubic model I want to mention only the application in the absorption on monolayers (Schick 1983), because these are two-dimensional effects and all calculations presented in this paper are also performed in two dimensions. The discrete cubic model can be used to describe the orientational ordering of diatomic molecules on a triangular lattice (Harris and Berlinsky 1979). Such a behaviour is observed in the absorption of N_2 molecules on a graphite surface (Chang and Dash 1977, Eckert *et al* 1979, Diehl *et al* 1983). Also the magnetic ordering of planar spins on a triangular lattice can be explained with the help of the cubic model (Domany and Riedel 1978).

The paper is organised as follows. In § 2 I shall present the model and show its place in the classification of a general Hamiltonian. This will demonstrate the connection with previously studied models. Also special cases and known results are presented. The predictions of the theory of conformal invariance are given in § 3. Section 4 briefly describes the numerical method used in this paper. As a first physical result the calculation of the critical point obtained by following RG trajectories is presented in § 5. In § 6 the critical exponents are derived and compared with the predictions of § 3. Finally § 7 contains my conclusions.

2. The cubic model

In this section the cubic model is described as a special case of a general Hamiltonian and known results of the model are presented. Let me start the classification with the most general Hamiltonian which has at least $\mathscr{Z}_6$ symmetry ($\mathscr{Z}_6 = \mathscr{Z}_2 \otimes \mathscr{Z}_3$):

$$-H = \sum_{\langle i,j \rangle} \{a_{0,0} + a_{1,0}(-1)^{\Delta\alpha} + a_{0,1}\omega^{\Delta\beta} + a_{1,1}(-1)^{\Delta\alpha}\omega^{\Delta\beta} + a_{0,2}\omega^{2\Delta\beta} + a_{1,2}(-1)^{\Delta\alpha}\omega^{2\Delta\beta}\} \quad (1)$$

where the lattice variables α_i and β_i of the lattice site i can have the following values:

$$\alpha_i \in \{0, 1\} \qquad \text{and} \qquad \beta_i \in \{0, 1, 2\}$$

and the interaction is composed of the multiplication of an Ising term $(-1)^{n\Delta\alpha}$ with $n \in \mathscr{Z}_2$ and a cubic term $\omega^{m\Delta\beta}$ with $m \in \mathscr{Z}_3$ where $\omega = \exp(2\pi i/3)$. The classification of the higher symmetries of the Hamiltonian in equation (1) which appear if some relations between the coupling constants $a_{n,m}$ are fulfilled has been done by Marcu *et*

al (1981). The results are shown in table 1. There $\mathscr{Z}_N$ denotes the cyclic group and analogue $\mathscr{S}_N$, the permutation group of N elements. The symbol $\mathscr{G} \wr \mathscr{H}$ represents the wreath product and the symbol $\mathscr{G} \otimes \mathscr{H}$ the direct product of the groups $\mathscr{G}$ and $\mathscr{H}$. Furthermore in the following a system is called a $\mathscr{G}$ model if it is invariant under a certain finite group $\mathscr{G}$.

From the models in table 1 the $\mathscr{S}_6$ model corresponds to the Potts model for $q = 6$ (Potts 1952). The $\mathscr{Z}_2 \otimes \mathscr{S}_3$ model has been studied by Domany and Riedel (1979) and therefore it is known as the Domany-Riedel model. It contains as a special case the vector Potts model.

In this paper I shall concentrate on the $\mathscr{Z}_2 \wr \mathscr{S}_3$ model. Introducing the coupling constants $C_1 = a_{0,1} = a_{0,2}$ and $C_2 = a_{1,0} = a_{1,1} = a_{1,2}$ and using the identities

$$1 + (-1)^{\alpha} = 2\delta(\alpha) \qquad \text{for} \qquad \alpha \in \{0, 1\}$$

and

$$1 + \exp(\tfrac{2}{3}\pi i\beta) + \exp(\tfrac{4}{3}\pi i\beta) = 3\delta(\beta) \qquad \text{for} \qquad \beta \in \{0, 1, 2\}$$

the Hamiltonian of the discrete cubic model can be written like

$$-H = \sum_{\langle i,j \rangle} C_1(3\delta(\Delta\beta) - 1) + C_2 3\delta(\Delta\beta)(2\delta(\Delta\alpha) - 1). \tag{2}$$

This Hamiltonian includes as special cases the Ising model ($C_1 \to \infty$), the Potts model for $q = 3$ ($C_2 = 0$), the Potts model for $q = 6$ ($C_1 = C_2$) and the cubic model in the form in which it has been initially defined by Kim *et al* (1975) ($C_1 = 0$). For the following I shall restrict myself to ferromagnetic interactions. In figure 1 the phase diagram is presented for the model given by the Hamiltonian in equation (2). It shows three different phases.

(i) The ordered (ferromagnetic) phase (C_2 large enough). All the lattice variables are fixed.

(ii) The partial ordered phase (C_2 small and C_1 large). Only the β_i are fixed. There is no constraint for the α_i.

(iii) The non-ordered (paramagnetic) phase (C_1, C_2 small). None of the variables is fixed.

Table 1. Classification of the general Hamiltonian with at least $\mathscr{Z}_6$ symmetry into higher symmetries and the corresponding relations between the coupling constants.

Global symmetry	Order of the group	Relation between the coupling constants
$\mathscr{Z}_2 \otimes \mathscr{Z}_3$	6	—
$\mathscr{Z}_2 \otimes \mathscr{S}_3$	12	$a_{0,1} = a_{0,2}$ $a_{1,1} = a_{1,2}$
$\mathscr{Z}_3 \wr \mathscr{Z}_2$	18	$a_{0,1} = a_{1,1}$ $a_{0,2} = a_{1,2}$
$\mathscr{Z}_2 \wr \mathscr{Z}_3$	24	$a_{1,0} = a_{1,1} = a_{1,2}$
$\mathscr{Z}_2 \wr \mathscr{S}_3$	48	$a_{0,1} = a_{0,2}$ $a_{1,0} = a_{1,1} = a_{1,2}$
$\mathscr{S}_3 \wr \mathscr{Z}_2$	72	$a_{0,1} = a_{0,2}$ $= a_{1,1} = a_{1,2}$
$\mathscr{S}_6$	720	$a_{1,0} = a_{0,1}$ $= a_{0,2} = a_{1,1} = a_{1,2}$

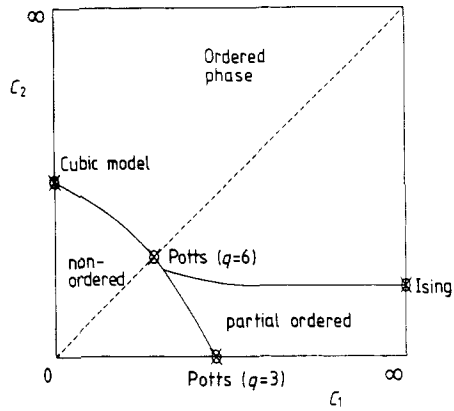

Figure 1. Phase diagram of the discrete cubic model with $\mathscr{Z}_2 \wr \mathscr{S}_3$ symmetry in the plane of the coupling constants C_1 and C_2. There are three different phases: the ordered phase, the partial ordered phase and the non-ordered phase. The phase transitions between the different phases are indicated by the full curves. Exactly known critical points which correspond to a certain choice of the coupling constants C_1 and C_2 are marked by the symbol ⊠ and labelled by the name of the models they belong to. The broken line ($C_1 = C_2$) is drawn to guide the eye.

The order of the phase transition and the critical exponents are only known for the special points which have already been mentioned. For the Ising case and the Potts case there are second-order phase transitions with critical exponents ($\alpha = 0$, $\eta = \frac{1}{4}$) and ($\alpha = \frac{1}{3}$, $\eta = \frac{4}{15}$) respectively. It is believed that the critical lines starting at these phase transition points meet somewhere before the third known point, the first-order phase transition of the Potts(6) model, is reached. The nature of the cubic transition between the ordered and the non-ordered phase is still the subject of intensive investigations. There are controversial contributions to this problem: Kim *et al* found a second-order phase transition in a mean-field calculation (Kim *et al* 1975) and a phase transition of first order using the Bethe-Peierls-Weiss approximation (Kim and Levy 1975). These calculations are both done for the case $C_1 = 0$. Nienhuis *et al* who applied a variational RG technique (Nienhuis *et al* 1983) published the result that the complete critical line of the cubic transition from $C_1 = 0$ to $C_1 = C_2$ is of first order. On the other hand we found a second-order phase transition (with $\nu \approx \frac{2}{3}$) (Badke *et al* 1985a) for the cases $C_1 = 0$ and $C_1 = 0.1$, $C_2 = 0.29$ in a Monte Carlo simulation combined with a finite-size scaling study (Barber 1983). Also in the Hamilton formulation of the model which will be introduced in the next section, the results are controversial. In this paper the results of a MCRG investigation of the model starting at the 'unknown' boundary of the phase diagram ($C_1 = 0$) are presented.

3. Predictions from conformal invariance

Recently the theory of conformal invariance has become an important tool in the classification of the universal critical behaviour in two dimensions. Based on the assumption that there is conformal invariance additional to the usual scale invariance at the critical point of a continuous phase transition, all critical exponents and multi-point correlation functions at the critical point can be obtained (for a review see

Cardy (1987)). They are connected to the representations of the underlying Virasoro algebra which is given by the following commutation relations:

$$[L_m, L_n] = (m-n)L_{m+n} + \tfrac{1}{12}cm(m^2-1)\delta_{m,-n} \tag{3}$$

where $n, m \in \mathscr{Z}$. Here c is the so-called conformal anomaly. If a system is conformal invariant and corresponds to a certain central charge $c \leqslant 1$ of the Virasoro algebra (Belavin *et al* 1984a, b, Friedan *et al* 1984) and if we also require unitarity, then the anomalous dimensions Δ_α and $\bar{\Delta}_\alpha$ which are defined by the two-point correlation function

$$\langle \Phi_\alpha(z_1, \bar{z}_1)\Phi_{\alpha'}(z_2, \bar{z}_2)\rangle = \delta_{\alpha\alpha'}(z_1 - z_2)^{-2\Delta_\alpha}(\bar{z}_1 - \bar{z}_2)^{-2\bar{\Delta}_\alpha} \tag{4}$$

where $z = x + \mathrm{i}y$ and $\bar{z} = x - \mathrm{i}y$ with x, y = coordinates of the plane are rational numbers:

$$\Delta_{p,q} = \frac{[(m+1)p - mq]^2 - 1}{4m(m+1)} \qquad (1 \leqslant p \leqslant m-1 \text{ and } 1 \leqslant q \leqslant m) \tag{5}$$

and the conformal anomaly is parametrised by:

$$c = 1 - \frac{6}{m(m+1)} \qquad m = 3, 4, \ldots . \tag{6}$$

The scale dimension x_α of an operator Φ_α is defined by:

$$x_\alpha = \Delta_\alpha + \bar{\Delta}_\alpha. \tag{7}$$

The main problem is the identification of a certain physical model with a fixed central charge and the corresponding representations of the Virasoro algebra.

Using the results of Cardy (1984a, b) and von Gehlen *et al* (1986) one can investigate the cubic model in the formulation of a finite quantum chain. von Gehlen and Rittenberg found conformal invariance and a second-order phase transition by measuring the finite-size scaling amplitudes for three different values of the coupling constant ε (von Gehlen and Rittenberg 1986, 1987). They calculated a central charge of $c \approx 1.25$ for all three points. Additionally they discovered a $N = 1$ supersymmetry for the point $\varepsilon = 0$. This makes it possible to find again a quantisation of the anomalous dimensions.

The supersymmetric generalisation of the Virasoro algebra which includes the additional odd generators G_r obeys the following commutation relations (Eichenherr 1985, Bershadsky *et al* 1985, Friedan *et al* 1985, Goddard *et al* 1985):

$$[L_m, L_n] = (m-n)L_{m+n} + \tfrac{1}{8}\tilde{c}(m^3 - m)\delta_{m,-n} \tag{8}$$

$$\{G_r, G_s\} = 2L_{r+s} + \tfrac{1}{2}\tilde{c}(r^2 - \tfrac{1}{4})\delta_{r,-s} \tag{9}$$

$$[L_m, G_r] = (\tfrac{1}{2}m + r)G_{m+r}. \tag{10}$$

The superconformal anomaly $\tilde{c}$ is connected to the usual conformal anomaly

$$\tilde{c} = \tfrac{2}{3}c. \tag{11}$$

The unitarity constraint gives the following formulae for the anomalous dimensions of the operators in the case of $\tilde{c} \leqslant 1$ (Friedan *et al* 1985, Goddard *et al* 1985):

$$\Delta_{p,q} = \frac{[p(\tilde{m}+2) - q\tilde{m}]^2 - 4}{8\tilde{m}(\tilde{m}+2)} + \tfrac{1}{32}[1 - (-1)^{p-q}] \tag{12}$$

with

$$\tilde{c} = 1 - \frac{8}{\tilde{m}(\tilde{m}+2)} \qquad \tilde{m} = 2, 3, 4, \ldots \tag{13}$$

and

$$1 \leqslant p < \tilde{m} \qquad 1 \leqslant q < \tilde{m} + 2. \tag{14}$$

The special case of the cubic model in the formulation of a quantum chain with the self-duality constraint corresponds for $\varepsilon = 0$ to a superconformal anomaly of (von Gehlen and Rittenberg 1986, 1987):

$$\tilde{c} = \tfrac{5}{6} \qquad (c = \tfrac{5}{4}). \tag{15}$$

The parameter which characterises the representations is given by $\tilde{m} = 6$ and the corresponding representations of the superconformal algebra belong to the Neveu-Schwarz sector (Neveu and Schwarz 1971) and are labelled by:

$$(\tfrac{1}{4})_{\mathrm{NS}} = (\tfrac{1}{4}, \tfrac{3}{4})_{\mathrm{VIR}} \qquad (0)_{\mathrm{NS}} = (0, \tfrac{3}{2})_{\mathrm{VIR}}. \tag{16}$$

From the pairs of the anomalous dimensions one derives the following scale dimensions for the neutral operators:

$$x_\alpha = \Delta_\alpha + \bar{\Delta}_\alpha$$

therefore:

Δ	$\bar{\Delta}$		x
$\frac{1}{4}$	$\frac{1}{4}$	$\rightarrow$	$\frac{1}{2}$
$\frac{3}{4}$	$\frac{3}{4}$	$\rightarrow$	$\frac{3}{2}$
$\frac{3}{2}$	$\frac{3}{2}$	$\rightarrow$	3

(17)

These scale dimensions give the critical exponents for the special kind of model constructed by Zamolodchikov and Fateev and also coincide with most of the known results from finite quantum chains. I shall derive the corresponding critical exponents in the Lagrange formulation of the cubic model to test the universality of the conjectured values.

4. The numerical method

In this section I shall briefly describe how the MCRG method has been implemented to achieve the results of the following sections.

The combination of the RG ansatz (Ma 1976) and the MC method leads to the powerful MCRG method (for a review see Swendsen 1982). In the framework of this method, procedures are available to estimate the critical point as well as to calculate critical exponents. Because these procedures are limited to cases where the fixed point of the theory is not too far away from the starting point it has been very important that, based on an idea of Callen (1963), methods have been developed to calculate effective renormalised coupling constants (Swendsen 1984a, b, Gupta and Cordery 1984). With the help of these kinds of calculations it is possible to follow the RG trajectories in the space of coupling constants. In this work I used the procedure of Swendsen (1984a, b) because of its better convergence properties (Shankar 1985).

One of the serious bottlenecks of the MCRG method is the fact that one has to use very large lattices in the MC simulation to be able to perform a reasonable number of block transformations. Here I have used a systematic enlargement procedure to avoid this problem (Badke 1987). Starting with a linear lattice size L one computes the effective renormalised coupling constants after a fixed number n of RG transformations. The actual linear lattice size is now L/b^n where b is the blocking factor. Then the lattice is enlarged to its original linear size L again and one performs a new simulation with the effective renormalised coupling constants. This procedure can be iterated to get as close as possible to the fixed point. In the method to calculate effective renormalised coupling constants there is a criterion which provides us with an estimate of the validity range of the iteration of the enlargement. The finite-size effects which finally limit the iteration turn out to be small (see § 6).

All the simulations in this work are performed on two-dimensional square lattices with periodic boundary conditions (for a review of the MC simulation see Binder (1979, 1984)). The linear lattice size of the start lattices varies from 16 to 64. Before the measurements I did at least as many thermalisation sweeps as measurement sweeps. Two successive measurements are separated by fifteen intermediate sweeps. For the production of random numbers a shift-register-generator with a period of $2^{250}-1$ has been used. This kind of pseudo-random number generator proves to be more suitable than the usual congruential generators if a huge amount of random numbers is required.

The RG transformations are performed with a blocking factor of $b=2$. This gives exactly four possibilities to choose the origin of the block transformation. The origin is permuted randomly in the transformation to increase the quality of the statistics especially at higher blocking levels. In the determination of the block spins I applied the majority rule. If the variables in the block under consideration are equally distributed, one of them is chosen randomly to be the new block spin.

5. The critical point

This section is separated into two parts. In the first I shall present the space of coupling constants which has been used and in the second the extracted result for the critical point is given.

To be able to detect first-order phase transitions some authors claim that it is necessary to allow vacancies in the RG transformation (Nienhuis *et al* 1983). Then the model under consideration transforms into the corresponding lattice-gas model. But the use of vacancies has not shown much success in the context of the MCRG approach (Rebbi and Swendsen 1980). In spite of the introduction of vacancies Rebbi and Swendsen were not able to see a clear difference between the second-order phase transition of the Potts model for $q=3,4$ and the first-order transition for $q=6,7$. Moreover a second-order phase transition can be driven to first order by choosing the coupling constant for the vacancy part in the Hamiltonian too large.

Instead of the introduction of vacancies I shall allow a space of coupling constants with a greater symmetry. To take into account all possible phase transitions of the cubic model (see figure 1) the Hamiltonian of equation (2) is divided into the following parts:

an Ising part

$$S_3^I = \sum_{f_I(i,j)} 2\delta(\Delta\alpha) - 1$$

a Potts part

$$S_1^l = \sum_{f_l(i,j)} 3\delta(\Delta\beta) - 1$$

a cubic part

$$S_2^l = \sum_{f_l(i,j)} (2\delta(\Delta\alpha) - 1)(3\delta(\Delta\beta) - 1). \tag{18}$$

The function f_l fixes the lattice variables which interact with each other. The different possible combinations are parametrised by l. In test measurements I found that the interactions which include more than two lattice variables give a contribution which cannot be separated from zero inside the error bars. Therefore I allowed only neighbour interactions. All interactions up to the fifth neighbours are included. The Hamiltonian which is used to analyse the renormalised configurations has the form:

$$-H = \sum_{l=0}^{4} \sum_{m=1}^{3} K_{3l+m} S_m^l \tag{19}$$

where l, m are the summation indices for the members and the parts of the interaction respectively. Table 2 gives a complete list of all coupling constants and their meaning.

Table 2. Overview of the fifteen coupling constants which are included in the analysis of the renormalised configurations. The dependence on the part and on the members of the interaction is shown.

Members of the interaction	Part of the interaction	S_1^l	S_2^l	S_3^l
Nearest neighbours	$l=0$	K_1	K_2	K_3
Second neighbours	$l=1$	K_4	K_5	K_6
Third neighbours	$l=2$	K_7	K_8	K_9
Fourth neighbours	$l=3$	K_{10}	K_{11}	K_{12}
Fifth neighbours	$l=4$	K_{13}	K_{14}	K_{15}

The starting point for the calculation of the critical exponents will be the critical point at the boundary $C_1 = 0$ in the phase diagram (see figure 1). This point is not analytically known and will now be determined with great precision. This is done by following the RG trajectories in the space of coupling constants. In detail:

two values of C_2 are chosen such that $C_2^1 \leqslant C_2^2$ and a MC simulation is performed for each of them;

effective renormalised coupling constants are calculated and the two corresponding RG trajectories are constructed;

if the trajectories move apart as shown in figure 2 then the wanted critical point lies between the chosen coupling constants:

$$C_2^1 \leqslant C_2^{\text{critical}} \leqslant C_2^2. \tag{20}$$

A new choice of C_2^1 and C_2^2 and a repetition of the calculation leads to a better localisation of the critical point.

This part of the calculation is performed on a 32^2 lattice with at least 5×10^4 measurements for each simulation. Because there are already some values available for the critical point (Kim *et al* 1975, Badke *et al* 1985a, b) it is possible to choose the first pair of coupling constants quite close together. The coupling constants of all the simulations which have been performed are listed in table 3.

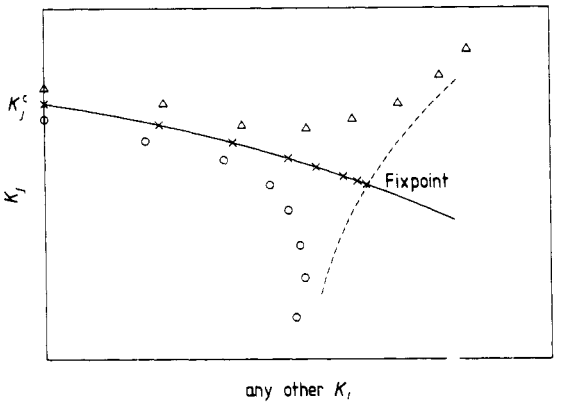

Figure 2. Schematic diagram for the renormalisation flows in the many-dimensional space of coupling constants under a typical renormalisation group transformation. The vertical axis represents the only non-zero coupling constant at the critical start point K_j^c, and the horizontal axis represents all other coupling constants generated by the transformation. The instability of the fixed point to perturbations out of the critical surface is indicated by ○ and △ (Swendsen 1982).

Table 3. Selection of the start coupling constants which are used in the localisation of the critical point of the cubic model. The notation corresponds to the one of the Hamiltonian defined in equation (19) with the coupling constants of table 2.

K_2^1	=	K_3^1	=	0.36						
		K_2^1	=	K_3^1	=	0.364				
				K_2^1	=	K_3^1	=	0.366		
						K_2	=	K_3	=	0.3665
				K_2^2	=	K_3^2	=	0.367		
		K_2^2	=	K_3^2	=	0.368				
K_2^2	=	K_3^2	=	0.37						

and $K_i^1 = K_j^1 = 0 \; \forall i \wedge \forall j > 2$

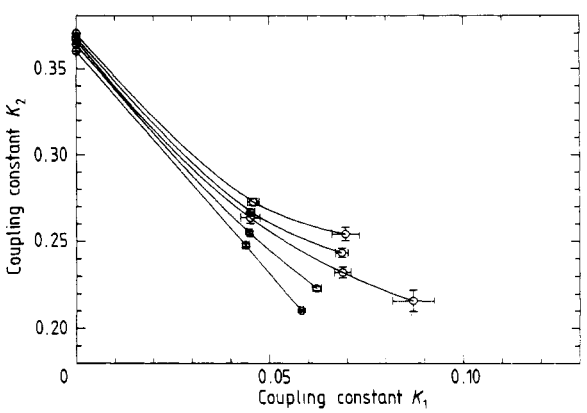

Figure 3. Renormalisation group trajectories in a projection of the fifteen-dimensional space of the effective renormalised coupling constants to a plane which is defined by K_1 and K_2. The values of five different start combinations of the coupling constants for a 32×32 lattice are shown.

Figure 3 shows the resulting RG trajectories for five selected start combinations in a projection of the fifteen-dimensional space of coupling constants to the two-dimensional plane which is defined by K_1 and K_2. The schematic behaviour of figure 2 is reproduced. To show the relations of the RG trajectories among each other in greater detail figure 4 contains the same values again, but for the values of K_2 I always subtracted the value of the central trajectory of figure 3. Hence figure 4 shows the deviations from the central trajectory in figure 3 with respect to the coupling constant K_2. The other projections of the fifteen-dimensional space to two-dimensional planes show analogous results.

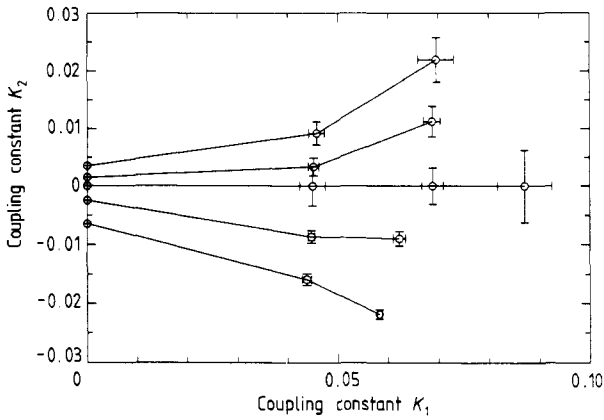

Figure 4. Renormalisation group trajectories in a projection of the fifteen-dimensional space of the effective renormalised coupling constants to a plane which is defined by K_1 and K_2. The values of five different start combinations of the coupling constants for a 32×32 lattice are shown. The values of K_2 indicate the deviation from the central trajectory of figure 3.

A close look at the numbers obtained gives another interesting observation. The relation $K_2 = K_3$ in the initial couplings is preserved in the effective renormalised coupling constants. In fact all the numbers on the first and second blocking level support a relation $K_{3l+2} = K_{3l+3}$ for $l = 0, 1, 2, 3, 4$. There is no splitting of the cubic interaction into the parts of the interaction of the Domany-Riedel model. This means also that at the fixed point which is approached by a RG transformation of this kind no isolated Ising part of the interaction will show up.

By the localisation of table 3 the critical point of the cubic model of Kim *et al* is determined to be

$$C_2^{\text{critical}} = (K_2 = K_3) = 0.3665 \pm 0.0005. \tag{21}$$

The error of this value is about one magnitude smaller than that of results published so far. This value is chosen to be the starting point for the calculation of critical exponents.

6. Critical exponents

This section describes the calculation of the critical exponents, the extrapolation to the fixed point and the comparison with known results and the predictions from conformal invariance.

The critical exponents are given by the eigenvalues of the transition matrix which is determined by a system of linear equations produced by the chain rule (Swendsen 1982). I performed simulations for the following lattice sizes:

start lattices of the size	64×64, 32×32, 16×16
once enlarged lattices of the size	64×64, 32×32, 16×16
twice enlarged lattices of the size	32×32, 16×16.

The results which will follow are extracted from 1.2×10^5 measurements for the 16×16 and the 32×32 lattice and from 0.7×10^5 measurements for the 64×64 lattice. The RG transformations are performed up to a 4×4 lattice. The transformation to a 2×2 lattice has been dropped because of the strong fluctuations involved. The critical exponents which I found are listed in tables 4 and 5. The diagonalisation of the transition matrix is done in five steps. The inclusion of all interaction parts of a certain combination of interaction members forms one step. A permutation of the order of the interaction combinations leads to the conclusion that the order chosen represents the significance of the interaction combinations in the right way. The contribution from the fifth-neighbour interaction is not relevant in most cases.

To study the finite-size effects one has to read tables 4 and 5 horizontally. If one calculates the differences of the values of the critical exponents in the rows of the tables one finds that the differences of the critical exponents which are caused by the finite size of the various lattices decrease with the number of operators included in the diagonalisation of the transition matrix. This behaviour allows the conclusion that

Table 4. Critical exponents y_T for different start lattice sizes with dependence on the blocking level n ($T_{\alpha\beta} = K_\alpha^{(n+1)}/K_\beta^{(n)}$) and on the rank of the transition matrix used in the analysis which is equal to the number of the included operators.

Blocking level n	Rank of $T_{\alpha\beta}$	Lattice size		
		64×64	32×32	16×16
0	3	1.139 (5)	1.132 (4)	1.131 (9)
	6	1.179 (6)	1.174 (6)	1.179 (9)
	9	1.180 (7)	1.175 (6)	1.181 (8)
	12	1.180 (7)	1.176 (6)	1.181 (8)
	15	1.180 (7)	1.176 (7)	1.180 (9)
1	3	1.199 (4)	1.191 (5)	1.194 (7)
	6	1.225 (4)	1.221 (7)	1.230 (8)
	9	1.226 (4)	1.224 (8)	1.23 (1)
	12	1.226 (4)	1.224 (9)	1.23 (1)
	15	1.226 (6)	1.225 (8)	1.23 (1)
2	3	1.241 (5)	1.233 (8)	
	6	1.262 (7)	1.259 (8)	
	9	1.265 (8)	1.26 (1)	
	12	1.26 (1)	1.26 (1)	
	15	1.26 (1)	1.26 (1)	
3	3	1.27 (1)		
	6	1.29 (1)		
	9	1.30 (2)		
	12	1.30 (2)		
	15	1.30 (2)		

Table 5. Critical exponents y_T for once enlarged lattices of different sizes with dependence on the blocking level $n(T_{\alpha\beta} = K_\alpha^{(n+1)}/K_\beta^{(n)})$ and on the rank of the transition matrix used in the analysis which is equal to the number of included operators.

Blocking level n	Rank of $T_{\alpha\beta}$	Lattice size		
		64×64	32×32	16×16
0	3	1.25 (1)	1.245 (5)	1.239 (6)
	6	1.266 (7)	1.263 (5)	1.264 (6)
	9	1.266 (7)	1.262 (7)	1.265 (8)
	12	1.266 (8)	1.261 (7)	1.264 (7)
	15	1.266 (9)	1.261 (8)	1.264 (6)
1	3	1.30 (1)	1.301 (7)	1.291 (4)
	6	1.321 (9)	1.317 (6)	1.313 (4)
	9	1.321 (9)	1.318 (6)	1.316 (7)
	12	1.32 (1)	1.317 (7)	1.32 (1)
	15	1.32 (1)	1.316 (8)	1.32 (1)
2	3	1.35 (2)	1.342 (9)	
	6	1.36 (2)	1.35 (1)	
	9	1.36 (2)	1.35 (1)	
	12	1.36 (2)	1.35 (1)	
	15	1.36 (3)	1.35 (1)	
3	3	1.38 (3)		
	6	1.39 (7)		
	9	1.40 (7)		
	12	1.41 (7)		
	15	1.42 (6)		

the finite-size effects which have shown up are caused mainly by the limitation of the space of coupling constants.

For a comparison of the values from the start lattice and the values from the enlarged lattice one has to take into account that the start lattice has been transformed twice before the effective renormalised coupling constants, which are the input for the enlarged lattice, are calculated. Therefore the third block in table 4 (the values for $n=2$) corresponds to the first block in table 5 (the values for $n=0$) and so on. The differences of related values decrease with the number of operators included in the diagonalisation of the transition matrix. This is clear because these differences are caused by the different finite-size effects of the lattices. On the other hand the good agreement of the values from the start lattices with the values from the enlarged lattices gives us some confidence that all the relevant operators have been taken into consideration. If one had missed an important operator in the calculation of the effective renormalised coupling constants then there should be a systematic difference between the values from the initial and the enlarged lattice.

The critical exponents are given by the eigenvalues of the transition matrix at the fixed point. Therefore I have to perform an extrapolation to the fixed point from the values obtained so far. This extrapolation corresponds to the limit $n\to\infty$ where the Hamiltonian H converges to H^*. The approach to the fixed-point Hamiltonian H^* is controlled by the next-to-leading critical exponent ω. This suggests the following extrapolation formula (Pawley *et al* 1984):

$$y_T = a_1 + a_2 b^{-n\omega}. \tag{22}$$

The constants a_1 and a_2 are determined by a fit. Such a behaviour is expected for large enough n. Figures 5 and 6 show the values of the critical exponents as a function of 2^{-n}. It is clear that the extrapolation has to be modified to take into account the enlargement in a suitable way:

$$y_T = a_1 + a_2 b^{-[n+(\sum_{j=1}^{l} n_j)]\omega}. \tag{23}$$

Here I allow for the enlargement in the following way: the number of RG transformations performed before the actual enlargement is added to the actual number of block transformations. There l is the number of enlargements and n_j is the number of RG transformations before the enlargement labelled by j.

The result for the next-to-leading exponent ω is $\omega = 0.5$ (see below). In figures 7 and 8 the values for the leading critical exponents are plotted against $2^{-(n+2)/2}$. This should produce a linear dependence. The straight lines show the best fit to the data where I dropped the values for $n = 0, 1$ (n should be large) to exclude uncontrollable systematic errors. The fits represent the data in a remarkable way and lead to the

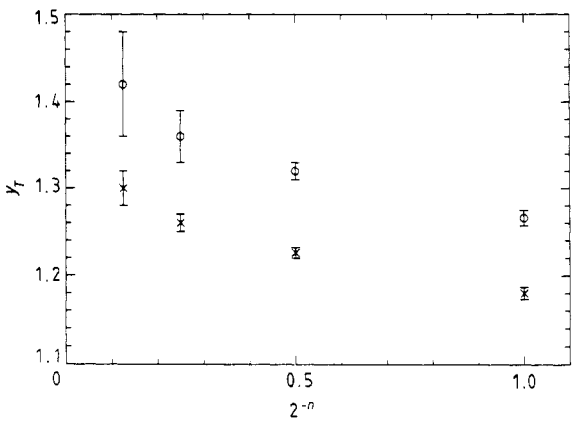

Figure 5. Measured critical exponents y_T with dependence on 2^{-n} for the 64×64 lattice. The blocking level is indicated by n and the values are marked by $\times$ for the original lattice and by $\bigcirc$ for the enlarged lattice.

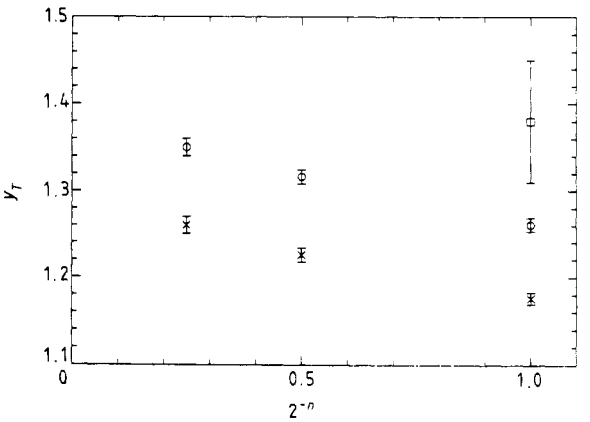

Figure 6. Analogous figure to figure 5 for the 32×32 lattice.

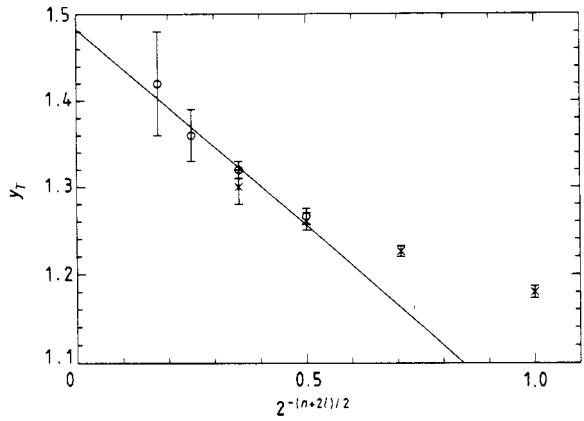

Figure 7. Measured critical exponents y_T with dependence on $2^{-(n+2l)/2}$ for the 64×64 lattice. The blocking level is indicated by n and the values are marked by $\times$ for the original lattice and by $\bigcirc$ for the enlarged lattice.

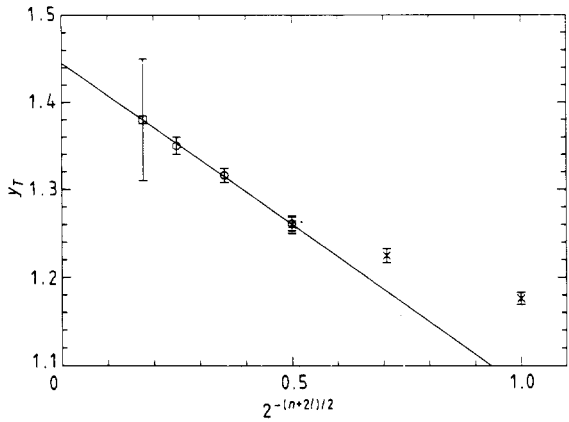

Figure 8. Analogous figure to figure 7 for the 32×32 lattice.

following final results for the critical exponents from the different lattices:

64×64-lattice	$y_T(\infty)=1.48\pm0.03$
32×32-lattice	$y_T(\infty)=1.44\pm0.01$
16×16-lattice	$y_T(\infty)=1.40\pm0.03.$

The quoted error bars correspond to one standard deviation in the fit in which the values are weighted by their individual errors.

For a first-order phase transition one would expect the leading exponent to be $y_T=2$. However, it has been found by other workers (Rebbi and Swendsen 1980 and references therein) that even if the phase transition is analytically known to be of first order, the value of the leading exponent is always about 10% smaller in MCRG studies. The numerical procedure applied here does not differ from the usual MCRG method in this point. But in spite of this systematic disadvantage of the MCRG method the pronounced difference between the obtained results and the first-order value leads to the conclusion that the cubic phase transition at $C_1=0$ is of second order. The values

of the leading exponent also suggest the following value for the critical exponent of the correlation length:

$$\nu = \frac{1}{y_T} = \frac{2}{3}. \tag{24}$$

The other thermal exponents can be obtained with the help of the scaling formulae.

A successive diagonalisation of the transition matrix produces, besides the leading eigenvalues, also the next eigenvalues which give the higher exponents. Unfortunately the finite-size effects increase in the calculation of these values. I report the values in tables 6 and 7. Without repeating the interpretation of the measured values which is discussed in detail for the leading exponent, I give the result for the second thermal exponent ω:

$$\omega = y_T^{(1)} = 0.5 \pm 0.1. \tag{25}$$

Note that the fits for the leading exponent do not change by more than a standard deviation if one chooses $\omega = 0.4$ or $\omega = 0.6$.

In determining the third exponent the limited statistics increases the error bars further. From table 8 I extracted the result of

$$y_T^{(2)} = -0.5 \pm 0.2 \tag{26}$$

with quite a large error. But the new value obtained is clearly different from zero. The value of the fourth exponent is around -1. Because of the strong fluctuations no definite results can be given.

Table 6. Higher critical exponents $\omega = y_T^{(1)}$ for different start lattice sizes with dependence on the blocking level $n(T_{\alpha\beta} = K_\alpha^{(n+1)}/K_\beta^{(n)})$ and on the rank of the transition matrix used in the analysis which is equal to the number of included operators.

Blocking level n	Rank of $T_{\alpha\beta}$	Lattice size		
		64×64	32×32	16×16
0	3	0.681 (7)	0.725 (6)	0.694 (6)
	6	0.713 (6)	0.723 (7)	0.733 (8)
	9	0.703 (8)	0.716 (7)	0.737 (8)
	12	0.685 (4)	0.718 (6)	0.735 (7)
	15	0.692 (5)	0.713 (6)	0.724 (8)
1	3	0.633 (5)	0.67 (3)	0.70 (4)
	6	0.64 (3)	0.66 (5)	0.68 (5)
	9	0.64 (3)	0.65 (5)	0.70 (3)
	12	0.64 (4)	0.66 (2)	0.70 (6)
	15	0.63 (4)	0.67 (3)	0.69 (4)
2	3	0.59 (4)	0.61 (5)	
	6	0.60 (6)	0.61 (4)	
	9	0.58 (5)	0.58 (5)	
	12	0.57 (3)	0.59 (5)	
	15	0.58 (5)	0.58 (7)	
3	3	0.57 (4)		
	6	0.58 (2)		
	9	0.56 (5)		
	12	0.56 (4)		
	15	0.56 (6)		

Table 7. Higher critical exponents $\omega = y_T^{(1)}$ for once enlarged lattices of different size with dependence on the blocking level $n(T_{\alpha\beta} = K_\alpha^{(n+1)}/K_\beta^{(n)})$ and on the rank of the transition matrix used in the analysis which is equal to the number of included operators.

Blocking level n	Rank of $T_{\alpha\beta}$	Lattice size		
		64×64	32×32	16×16
0	3	0.58 (3)	0.56 (3)	0.53 (6)
	6	0.57 (4)	0.58 (4)	0.59 (3)
	9	0.57 (4)	0.57 (4)	0.59 (3)
	12	0.56 (2)	0.57 (3)	0.60 (3)
	15	0.56 (3)	0.56 (4)	0.60 (4)
1	3	0.56 (5)	0.58 (3)	0.50 (4)
	6	0.56 (2)	0.56 (5)	0.58 (5)
	9	0.55 (3)	0.56 (5)	0.58 (3)
	12	0.56 (3)	0.56 (2)	0.57 (6)
	15	0.54 (3)	0.52 (3)	0.57 (4)
2	3	0.51 (4)	0.50 (5)	
	6	0.52 (4)	0.53 (5)	
	9	0.52 (5)	0.53 (6)	
	12	0.52 (4)	0.53 (5)	
	15	0.52 (5)	0.50 (6)	
3	3	0.54 (4)		
	6	0.53 (5)		
	9	0.52 (5)		
	12	0.51 (6)		
	15	0.51 (6)		

Table 8. Higher critical exponents $y_T^{(2)}$ for once enlarged lattices of different size with dependence on the blocking level $n(T_{\alpha\beta} = K_\alpha^{(n+1)}/K_\beta^{(n)})$ and on the rank of the transition matrix used in the analysis which is equal to the number of included operators.

Blocking level n	Rank of $T_{\alpha\beta}$	Lattice size		
		64×64	32×32	16×16
0	3	−0.51 (5)	−0.51 (7)	−0.37 (7)
	6	−0.32 (7)	−0.36 (7)	−0.42 (8)
	9	−0.36 (6)	−0.36 (6)	−0.38 (8)
	12	−0.34 (6)	−0.38 (8)	−0.41 (7)
	15	−0.37 (5)	−0.50 (8)	−0.41 (9)
1	3	−0.41 (6)	−0.38 (7)	−0.2 (1)
	6	−0.38 (6)	−0.29 (8)	−0.4 (1)
	9	−0.42 (7)	−0.35 (8)	−0.4 (1)
	12	−0.44 (7)	−0.36 (9)	−0.3 (1)
	15	−0.43 (9)	−0.36 (7)	−0.3 (1)
2	3	−0.4 (1)	−0.2 (1)	
	6	−0.5 (1)	−0.3 (2)	
	9	−0.4 (2)	−0.4 (2)	
	12	−0.5 (1)	−0.5 (1)	
	15	−0.5 (2)	−0.4 (2)	

After discussing the measurements in detail I now want to compare them with known results and predictions. From my MCRG study the following values for the first three thermal critical exponents of the cubic model are suggested:

$$y_T^{(0)}=1.5 \qquad y_T^{(1)}=0.5 \qquad y_T^{(2)}=-0.5 \tag{27}$$

and the phase transition is of second order. This conflicts with the results of Kim and Levy, Nienhuis *et al* and the Hamilton calculations of Iglói (1986). But there is agreement with our previous results and the ones of von Gehlen and Rittenberg. The value of the leading critical exponent is the same as in these investigations.

These critical exponents correspond to the following scale dimensions:

$$x_T^{(0)}=\tfrac{1}{2} \qquad x_T^{(1)}=\tfrac{3}{2} \qquad x_T^{(2)}=\tfrac{5}{2}. \tag{28}$$

An important observation is the fact that no marginal operator has been found. Because a scale dimension with a value greater than two has been identified the conjecture can be made that for the critical point under consideration no marginal operator exists at all. This means that the critical exponents are fixed in the Lagrange formulation of the model for the cubic transition.

Now I shall interpret the obtained scale dimensions with the help of the theory of conformal invariance. Therefore the measured values are compared with the predicted anomalous dimensions given in § 3. The first two scale dimensions are identified at once:

$$(\tfrac{1}{4},\tfrac{1}{4})_{\mathrm{VIR}} \rightarrow x_1=\Delta_1+\bar{\Delta}_1=\tfrac{1}{4}+\tfrac{1}{4}=\tfrac{1}{2}$$

$$(\tfrac{3}{4},\tfrac{3}{4})_{\mathrm{VIR}} \rightarrow x_2=\Delta_2+\bar{\Delta}_2=\tfrac{3}{4}+\tfrac{3}{4}=\tfrac{3}{2}.$$

The third representation $(\frac{5}{2},\frac{5}{2})_{\mathrm{VIR}}$ predicts a scale dimension of $x_3=3$ which is supported by the fourth critical exponent which was found to be near -1. A clear identification is not possible due to the large uncertainty of the measurement.

To find the place of the measured scale dimension of $x=\frac{5}{2}$ in the framework of the conformal invariance one has to remember that to each primary field with the scale dimension Δ there belongs a complete conformal tower (Belavin *et al* 1984a, b). All the operators on the Nth level of this tower have a scale dimension of $(\Delta+N)$. Hence the scale dimension of the operators in the first level of the conformal tower of the leading neutral operator is:

$$x_1^{(1)}=(1+\tfrac{1}{4})+(1+\tfrac{1}{4})=\tfrac{5}{2}. \tag{29}$$

This coincides with the scale dimension derived from the third critical exponent.

Table 9. Relation between the obtained numerical results for the critical exponents and the scale and anomalous dimensions and interpretation from the point of view of the corresponding operators.

n	$y_T^{(n)}$	$x_T^{(n)}$	$\Delta_{(n)}$	$\bar{\Delta}_{(n)}$	Interpretation
0	1.5	0.5	$\frac{1}{4}$	$\frac{1}{4}$	Lowest level of the neutral operator with anomalous dimension $(\frac{1}{4},\frac{1}{4})$
1	0.5	1.5	$\frac{3}{4}$	$\frac{3}{4}$	Lowest level of the neutral operator with anomalous dimension $(\frac{3}{4},\frac{3}{4})$
2	−0.5	2.5	$1+\frac{1}{4}$	$1+\frac{1}{4}$	First level of the conformal tower of the operator with anomalous dimension $(\frac{1}{4},\frac{1}{4})$

All the critical exponents obtained in the MCRG study support the identification of the cubic model with a superconformal anomaly of $\tilde{c} = \frac{5}{6}$ ($c = \frac{5}{4}$). The scale dimensions of the first and second neutral operator correspond to the leading and the next-to-leading thermal critical exponent. The third thermal critical exponent matches with the scale dimension of the first level of the conformal tower of the representation labelled by $(\frac{1}{4}, \frac{1}{4})$. The complete identification is presented in detail in table 9.

7. Conclusions

The aim of this paper was to test some new numerical features of the MCRG method on the one hand and to present some new results for the discrete cubic model on the other hand.

From the numerical point of view I showed that it is possible to extend the accuracy of the measurement of the critical point by following the RG trajectories, although one has to say that this procedure requires a lot of computer work. The systematic approach to the fixed point by the calculation of effective renormalised coupling constants is successfully combined with an extrapolation scheme for the critical exponents.

On the physical side the critical point of the cubic model in the special case of $C_1 = 0$ has been determined to be $C_2^{\text{critical}} = 0.3665 \pm 0.0005$. In the RG transformation no splitting of the cubic interaction has been found. This allows the conclusion that the critical starting point is moved by the RG transformation only on the plane of the cubic model.

The phase transition is of second order with a critical exponent of the correlation length of $\nu = \frac{2}{3}$. Between the higher critical exponents no marginal one is found. Therefore the critical exponents should not change on the cubic critical line.

All the higher exponents can be interpreted in the framework of the theory of superconformal invariance. The identification of a special point in the space of the coupling constants with a superconformal anomaly $\tilde{c} = \frac{5}{6}$ which has been suggested and found by von Gehlen and Rittenberg is supported by all the measured critical exponents.

To clarify the properties of the cubic phase transition completely, additional points on the cubic critical line should be investigated and also magnetic exponents should be taken into consideration. Another interesting question is the behaviour of the critical exponents in the neighbourhood of the first-order critical point at $C_1 = C_2$. To identify conformal anomalies the number of calculated critical exponents has to be increased. This might be possible if the MCRG method can be improved by an analytical treatment of the finite-size effects in the enlargement procedure.

Acknowledgments

It is a pleasure to thank E Katznelson and V Rittenberg for helpful and stimulating discussions.

References

Aharony A 1977 *J. Phys. A: Math. Gen.* **10** 389
Alcaraz F C 1986 *Canberra Research Report 31-1986*
Ashkin J and Teller E 1943 *Phys. Rev.* **64** 178

Badke R 1987 *Phys. Lett.* **119A** 365
Badke R, Reinicke P and Rittenberg V 1985a *J. Phys. A: Math. Gen.* **18** 73
—— 1985b *J. Phys. A: Math. Gen.* **18** 653
Barber M N 1983 *Phase Transitions and Critical Phenomena* vol 8, ed C Domb and J L Lebowitz (New York: Academic) p 145
Belavin A A, Polyakov A M and Zamolodchikov A B 1984a *J. Stat. Phys.* **34** 763
—— 1984b *Nucl. Phys.* B **241** 333
Bershadsky M A, Knizhnik V G and Teitelman M G 1985 *Phys. Lett.* **151B** 31
Binder K (ed) 1979 *Monte Carlo Methods in Statistical Physics, Topics in Current Physics* vol 7 (Berlin: Springer)
—— 1984 *Applications of the Monte Carlo Method, Topics in Current Physics* vol 36 (Berlin: Springer)
Callen H B 1963 *Phys. Lett.* **4** 161
Cardy J L 1984a *J. Phys. A: Math. Gen.* **17** L385
—— 1984b *Nucl. Phys.* B **240** 514
—— 1987 *Phase Transitions and Critical Phenomena* vol 11, ed C Domb and J L Lebowitz (New York: Academic) to be published
Chang T T and Dash J G 1977 *Surf. Sci.* **66** 559
Diehl R D, Taney M F and Fain S C Jr 1983 *Surf. Sci.* **125** 116
Ditzian R V, Banavar J R, Grest G S and Kadanoff L P 1980 *Phys. Rev.* B **22** 2542
Domany E and Riedel E K 1978 *Phys. Rev. Lett.* **40** 561
—— 1979 *Phys. Rev.* B **19** 5817
Eckert J, Ellenson W D, Hastings J B and Passell L L 1979 *Phys. Rev. Lett.* **43** 1329
Eichenherr H 1985 *Phys. Lett.* **151B** 26
Friedan D, Qiu Z and Shenker S 1984 *Phys. Rev. Lett.* **52** 1575
—— 1985 *Phys. Lett.* **151B** 37
Goddard P, Kent A and Olive D 1985 *Phys. Lett.* **152B** 88
Gupta R and Cordery R 1984 *Phys. Lett.* **105A** 415
Harris A B and Berlinsky A J 1979 *Can. J. Phys.* **57** 1852
Iglói F 1986 *J. Phys. A: Math. Gen.* **19** 563, 575
Kim D and Levy P M 1975 *Phys. Rev.* B **12** 5105
Kim D, Levy P M and Uffer L F 1975 *Phys. Rev.* B **12** 989
Ma S K 1976 *Phys. Rev. Lett.* **37** 461
Marcu M, Regev A and Rittenberg V 1981 *J. Math. Phys.* **22** 2740, 2753
Neveu A and Schwarz J H 1971 *Nucl. Phys.* B **31** 86
Nienhuis B, Riedel E K and Schick M 1983 *Phys. Rev.* B **27** 5625
Pawley G S, Wallace D J, Swendsen R H and Wilson K G 1984 *Phys. Rev.* B **29** 4030
Potts R B 1952 *Proc. Camb. Phil. Soc.* **48** 106
Rebbi C and Swendsen R H 1980 *Phys. Rev.* B **21** 4094
Schick M 1983 *Surf. Sci.* **125** 125
Shankar R 1985 *Yale preprint YTP 85-25*
Swendsen R H 1982 *Real Space Renormalisation, Topics in Current Physics* vol 30, ed Th W Burkhardt and J M J van Leeuwen (Berlin: Springer)
—— 1984a *Phys. Rev. Lett.* **52** 1165, 2321
—— 1984b *Phys. Rev.* B **30** 3866, 3875
von Gehlen G and Rittenberg V 1986 *J. Phys. A: Math. Gen.* **19** 2439
—— 1987 *J. Phys. A: Math. Gen.* **20** 227
von Gehlen G, Rittenberg V and Ruegg H 1986 *J. Phys. A: Math. Gen.* **19** 107
Zamolodchikov A B and Fateev V A 1985 *Zh. Eksp. Teor. Fiz.* **89** 380 (1985 *Sov. Phys.-JETP*) **62** 215